

Micron-sized fiber diamond probe for quantum precision measurement of microwave magnetic field

Wen-Tao Lu(卢文韬), Sheng-Kai Xia(夏圣开), Ai-Qing Chen(陈爱庆), Kang-Hao He(何康浩), Zeng-Bo Xu(许增博), Yi-Han Chen(陈艺涵), Yang Wang(汪洋), Shi-Yu Ge(葛仕宇),Si-Han An(安思瀚), Jian-Fei Wu(吴建飞), Yi-Han Ma(马艺菡), and Guan-Xiang Du(杜关祥)

Citation: Chin. Phys. B, 2024, 33 (**8**): 080305. DOI: 10.1088/1674-1056/ad5321
Journal homepage: http://cpb.iphy.ac.cn; http://iopscience.iop.org/cpb

What follows is a list of articles you may be interested in

Coexistence behavior of asymmetric attractors in hyperbolic-type memristive Hopfield neural network and its application in image encryption

Xiaoxia Li(李晓霞), Qianqian He(何倩倩), Tianyi Yu(余天意),Zhuang Cai(才壮), and Guizhi Xu(徐桂芝)
Chin. Phys. B, 2024, 33 (**3**): 030505. DOI: 10.1088/1674-1056/acf281

Projective representation of D_6 group in twisted bilayer graphene

Noah F. Q. Yuan
Chin. Phys. B, 2021, 30 (**7**): 070311. DOI: 10.1088/1674-1056/ac00a3

Zitterbewegung of Dirac quasiparticles emerged in a Su-Schrieffer–Heeger lattice

Yue Hu(胡玥), Zheng-Xin Guo(郭政鑫), Ze-Ming Zhong(钟泽明), and Zhi Li(李志)
Chin. Phys. B, 2020, 29 (**11**): 110302. DOI: 10.1088/1674-1056/abb45b

Analytical model of tilted driver-pickup coils for eddy current nondestructive evaluation

Bing-Hua Cao(曹丙花), Chao Li(李超), Meng-Bao Fan(范孟豹), Bo Ye(叶波), Gui-Yun Tian(田贵云)
Chin. Phys. B, 2018, 27 (**3**): 030301. DOI: 10.1088/1674-1056/27/3/030301

Inverse problem of pulsed eddy current field of ferromagnetic plates

Chen Xing-Le (陈兴乐), Lei Yin-Zhao (雷银照)
Chin. Phys. B, 2015, 24 (**3**): 030301. DOI: 10.1088/1674-1056/24/3/030301

Micron-sized fiber diamond probe for quantum precision measurement of microwave magnetic field

Wen-Tao Lu(卢文韬)[1], Sheng-Kai Xia(夏圣开)[2], Ai-Qing Chen(陈爱庆)[3], Kang-Hao He(何康浩)[3], Zeng-Bo Xu(许增博)[4], Yi-Han Chen(陈艺涵)[5], Yang Wang(汪洋)[6], Shi-Yu Ge(葛仕宇)[3], Si-Han An(安思瀚)[3], Jian-Fei Wu(吴建飞)[7], Yi-Han Ma(马艺菡)[3], and Guan-Xiang Du(杜关祥)[3,†]

[1] *Portland Institute, Nanjing University of Posts and Telecommunications, Nanjing* 210023, *China*
[2] *School of Computer Science, Nanjing University of Posts and Telecommunications, Nanjing* 210023, *China*
[3] *College of Telecommunication and Information Engineering, Nanjing University of Posts and Telecommunications, Nanjing* 210003, *China*
[4] *School of Economics, Nanjing University of Posts and Telecommunications, Nanjing* 210023, *China*
[5] *School of Electronic and Optical Engineering, Nanjing University of Posts and Telecommunications, Nanjing* 210023, *China*
[6] *School of Science, Nanjing University of Posts and Telecommunications, Nanjing* 210023, *China*
[7] *College of Electronic Science and Technology, National University of Defense Technology, Changsha* 410000, *China*

(Received 11 April 2024; revised manuscript received 30 May 2024; accepted manuscript online 3 June 2024)

We present a quantitative measurement of the horizontal component of the microwave magnetic field of a coplanar waveguide using a quantum diamond probe in fiber format. The measurement results are compared in detail with simulation, showing a good consistence. Further simulation shows fiber diamond probe brings negligible disturbance to the field under measurement compared to bulk diamond. This method will find important applications ranging from electromagnetic compatibility test and failure analysis of high frequency and high complexity integrated circuits.

Keywords: quantum precision measurement, electromagnetic field, diamond NV center, quantum metrology

PACS: 03.65.Yz, 52.70.Gw, 42.50.Ex **DOI:** 10.1088/1674-1056/ad5321

1. Introduction

The precision measurement and metrology of electromagnetic fields (EMF) is crucial for the design of communication systems, development of electronic devices, and understanding of physical phenomena. In order to achieve more accurate measurements and higher resolution, there has been an increasing requirement for probes. Traditional methods use small loop antennas[1] or PCB-based multi-layer microstrip lines to calculate the magnetic field intensity according to electromagnetic induction, so as to characterize the surface current and EMF of RF devices.[2] However, the spatial resolution of this method cannot be further optimized due to the size limitation of the probe itself.

Quantum precision measurement is gaining attention for its ability to break the standard quantum limit (SQL) of traditional methods and approach Heisenberg limit. Adaptation to extreme environments further enhances its utility and broadens its application. There are two commonly used quantum precision measurement methods of EMF: Rydberg atoms[3–5] and alkali atom vapor-cells. Rydberg atoms can measure AC electric fields based on the Autler–Townes (AT) effect, while alkali atom vapor-cells use Rabi oscillation to measure AC magnetic field. However, both methods have drawbacks that cannot be ignored. Rydberg atoms struggle to infer magnetic fields from single electric field data, while the disturbance to EMF by alkali atom vapor-cells cannot be ignored.[6]

In the measurement of microwave (MW) magnetic fields, an alternative is nitrogen-vacancy (NV) center, which can be excited and read out all-optically, using common equipment like confocal microscopes,[7] atomic force microscopes,[8] and CCDs.[9] Diamond's non-magnetic nature minimizes MW magnetic field disturbance, enhancing measurement accuracy. Advancements in quantum state control,[10–12] high-resolution imaging,[13,14] communication,[15] and optimization of pulse trains[16] and magnetic field phases[17] mark a steady evolution in NV center technology.

In this context, we propose a microwave magnetic field measurement method based on diamond NV center, and prove its disturbance to RF devices and electromagnetic fields. Our methodology unfolds in two key steps:

(i) Use a tapered fiber diamond probe to characterize the microwave magnetic field above the surface of a coplanar waveguide with micron-sized spatial resolution and high accuracy.

(ii) Compare the disturbance of two commonly used diamond structures: fiber diamond probe and bulk diamond on RF devices from two aspects of electromagnetic field and transmission characteristics through simulation.

Through experiments and simulations, our work demonstrates the feasibility and superiority of quantum precision measurement using NV center with fiber diamond probes.

†Corresponding author. E-mail: duguanxiang@njupt.edu.cn

© 2024 Chinese Physical Society and IOP Publishing Ltd

2. Basic theory and experimental results

Similar to alkali atom vapor-cells, the NV center measurement of MW magnetic field is also based on Rabi oscillation. In the absence of DC magnetic field, there is a zero-field split $D = 2.87$ GHz between $m_s = 0$ and $m_s = \pm 1$. When a DC magnetic field is applied, MW magnetic field drives Rabi oscillations between the $m_s = 0$ and $m_s = \pm 1$ states at resonance. The transitions between $m_s = 0$ and $m_s = \pm 1$ are driven by the left and right circular polarization $\sigma_\pm$ respectively,[17] as depicted in Fig. 1(a). The oscillation frequency is linearly proportional to the amplitude of MW magnetic field, as given by the following formula:

$$f_{\text{oscillation}} = \gamma_{\text{NV}} B_{\text{MW}}, \tag{1}$$

where $\gamma_{\text{NV}} = 2.802495$ MHz/Gs (1 Gs = 10^{-4} T) is the gyromagnetic ratio of the electron spin, B_{MW} denotes the circular polarization component of MW magnetic field projected in the plane perpendicular to the NV axis. On the surface of RF devices, electromagnetic waves usually exist in the form of linear polarization, which can be decomposed into two circularly polarized waves of equal amplitude and opposite rotations. Therefore, the amplitude of the original MW magnetic field can be obtained based on the amplitude calculated by Rabi oscillation.

The coplanar waveguide (CPW) is selected to be measured with a tapered fiber diamond probe (FDP), for its superior transmission properties and uniform EMF distribution. With a signal line width of 150 μm and gap width of 120 μm, the S parameter of CPW is shown in Fig. 1(b). Two commonly used forms of NV center, FDP and bulk diamond, are depicted in Figs. 1(c) and 1(d), with a defined coordinate system for clarity.

The FDP shown in Fig. 1(c) was used in the experiment. A green laser with a wavelength of 532 nm pumps the diamond crystal at the front taper through the fiber, and the red fluorescence is returned along the original path, passing through the dichroic mirror and entering the avalanche photodetector (APD) to output a voltage signal. We characterize the MW magnetic field with the NV axis set vertically,[18–20] and the Rabi frequency at resonance can reflect the horizontal component of MW magnetic field (composed of the X and Y components). The Zeeman effect splits energy levels under a DC magnetic field, representing four peaks in the optically detected magnetic resonance (ODMR) spectrum.[21] Typical ODMR spectrum and Rabi oscillation are shown in Figs. 2(a) and 2(b).

The horizontal component of MW magnetic field along the X and Z directions of the CPW is measured and compared against experimental results. The actual output power of the excitation source is confirmed at 23.43 dBm. As shown in Figs. 2(c) and 2(d), there is a close match between the simulation and measurement data, indicating accuracy in the experimental results.

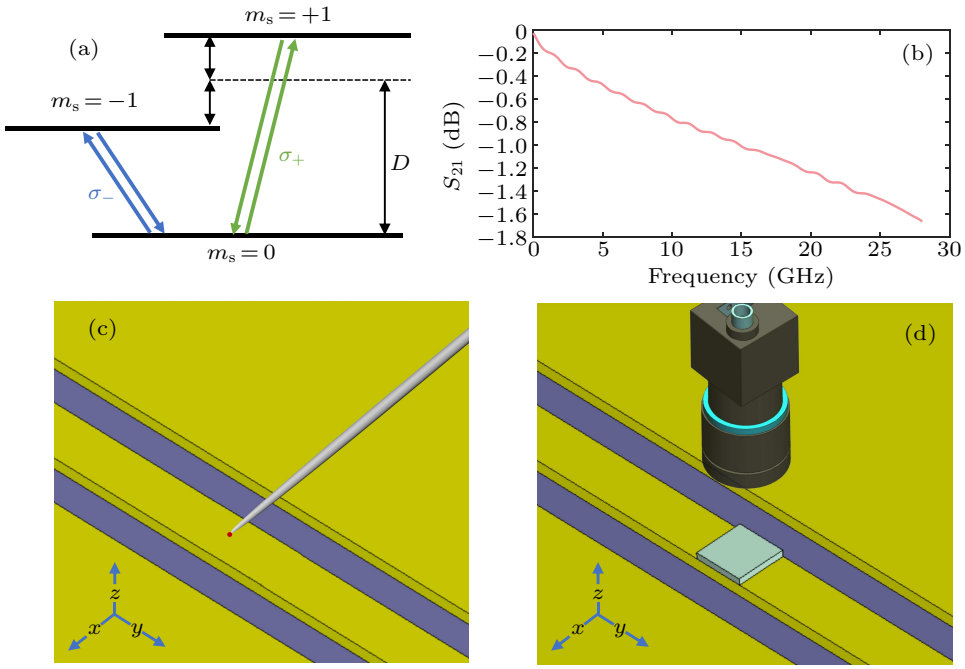


Fig. 1. (a) When there is no DC magnetic field, there is a zero-field split $D = 2.87$ GHz between $m_s = 0$ and $m_s = \pm 1$. According to the transition selection rules of dipoles, the transitions between the $m_s = 0$ and $m_s = \pm 1$ states are driven by the $\sigma_\pm$, circularly polarized components of the MW fields, respectively (σ_- stands for right circular polarization, while σ_+ stands for left circular polarization). (b) The S parameter of coplanar waveguide. Coplanar waveguide has stable and uniform electromagnetic characteristics in the wide band, and is used as a representative RF device in the experiments and simulations of this work. (c) Tapered fiber diamond probe. The red part of the figure represents NV center ensemble, which can reach submicron size and thus obtain submicron resolution. (d) Bulk diamond with confocal microscope and CCD camera. By taking pictures, two-dimensional (2D) field distribution can be quickly scanned.

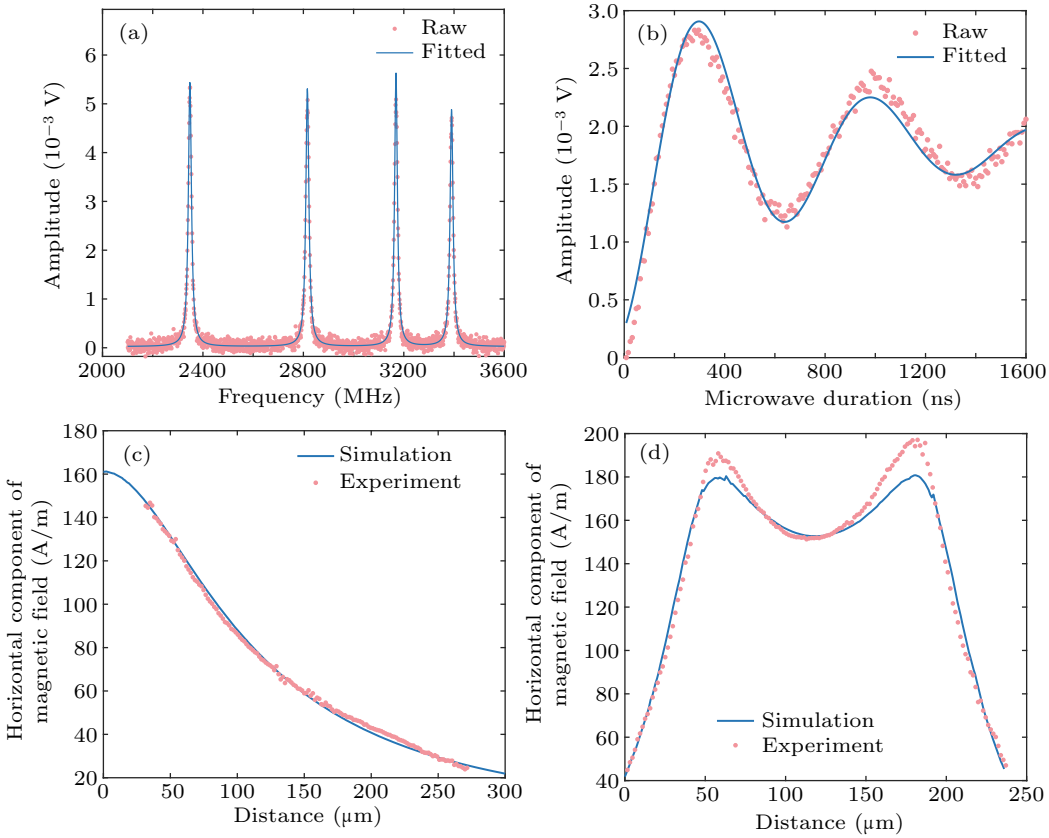


Fig. 2. (a) Typical ODMR spectrum showing four resonance peaks of NV center. The two outer peaks represent the well-oriented NV axis, and the frequency difference between the two peaks is proportional to the strength of the applied DC magnetic field. The two peaks in the middle are formed by overlapping the six peaks of the other three axes, which have equal angles to the DC magnetic field and thus equal frequencies of the peaks. (b) Typical Rabi oscillation. The fluorescence intensity of NV color center changes periodically with the increase of microwave duration. After the fluorescence signal enters the avalanche photodiode, it is reflected as a change in the output electric signal. (c) The distribution of the horizontal component of MW magnetic field above CPW in the Z direction at the frequency of 3.39 GHz. (d) The distribution of the horizontal component of MW magnetic field above CPW in the X direction at the frequency of 3.39 GHz (25 μm upper from the CPW's surface).

3. Simulation of two diamond structures

In quantum precision measurements of NV centers, bulk diamonds are widely used for its ability to achieve rapid 2D imaging. The 2D microwave field can be imaged in a short time by using confocal optical path and CCD camera. Such experiments do not require electric displacement tables and point-by-point scanning, which will greatly improve the efficiency, and do not need to consider the impact of environmental changes and other factors. But this requires contact with the RF device, which can affect sensitive electronics and limit 3D scanning in complex circuits. Our previous work introduces a tapered FDP[22,23] as an alternative, enabling submicron imaging without contact. Although more complex equipment and preparation process are required, as well as point-by-point scanning, which takes more time, it ensures the accuracy of the measurement. This approach offers high-resolution scanning adaptable to various scenarios. To compare the disturbance caused by these methods, we use Ansys HFSS 19.1 to simulate the MW magnetic field and transmission at the frequency of 5 GHz.

Initially, we concentrated on characterizing the MW magnetic field and transmission properties of RF devices disturbed by bulk diamonds. For this, we employ a 150 μm×150 μm×20 μm diamond cuboid with $\varepsilon_r = 5.7$ and $\mu_r = 1$. The CPW is placed in the same direction as stated in the previous section, with a feed power of 30 dBm.

The diamond's bottom aligns with the CPW's top, centered horizontally. Since CPW has extremely excellent transmission characteristics, it can be regarded as a uniform transmission line. In the direction of the transmission line, the electromagnetic characteristics can be considered to be equal everywhere, so our disturbance analysis focuses on a single reference line. In the simulation, a symmetrical line across the diamond's center is chosen. The disturbance is quantified by the rate of change (ROC), expressed as a percentage

$$\mathrm{ROC} = \left| \frac{H^{\mathrm{Diamond}}}{H^{\mathrm{Vaccum}}} - 1 \right| \times 100\%. \tag{2}$$

For the relatively large X component, we calculate the ROC along the specified reference line. As shown in Fig. 3(a), the bulk diamond induces a magnetic field disturbance of about 2%, a value noteworthy and not negligible in our analysis.

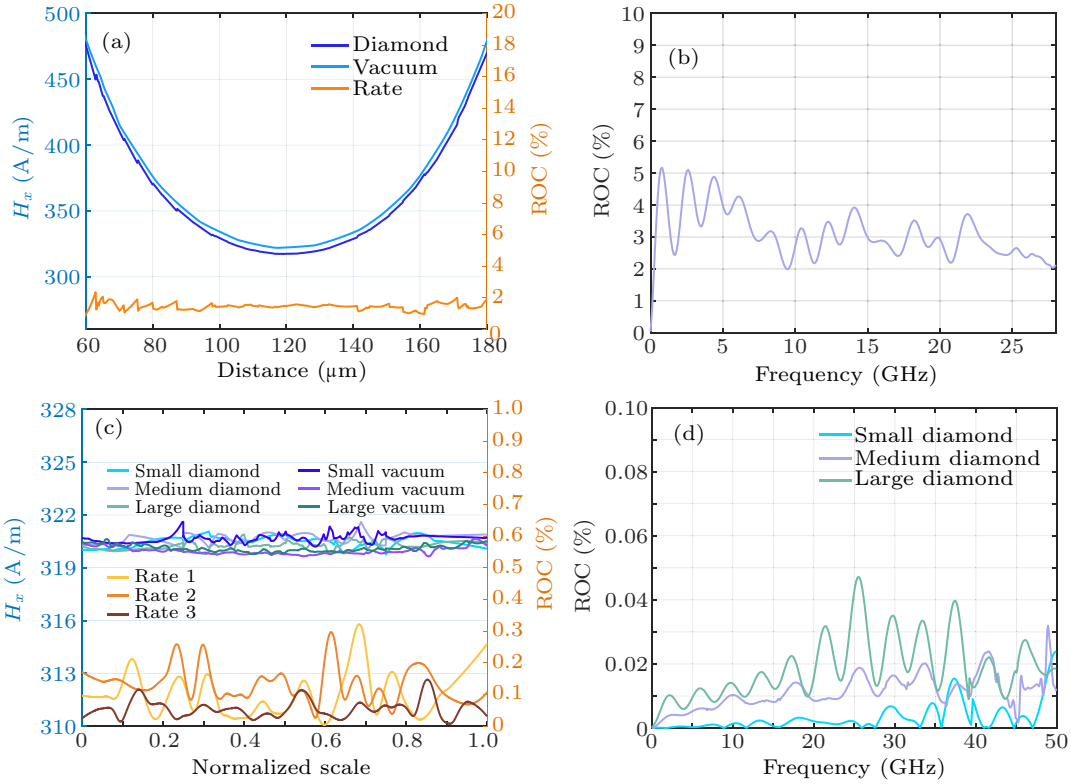


Fig. 3. (a) The amplitude of H_x before and after adding bulk diamond and the corresponding ROC. (b) The ROC of S_{21} after adding bulk diamond. (c) The amplitude of H_x before and after adding FDP and the corresponding ROC. (d) The ROC of S_{21} after adding FDP.

Regarding transmission properties, we evaluate the disturbance by monitoring changes of S_{21}. Figure 3(b) shows that at gigahertz frequencies, S_{21} varies by over 2%, indicating significant impedance mismatch due to the bulk diamond's direct contact with the CPW. This disturbs RF device's performance and EMF distribution, conflicting with the objectives of quantum precision measurement.

We proceed with an analysis of the FDP, noting tapered fiber structure's enhancement of fluorescence collection and efficient pumping.[22,23] For the simulation, we simplify the model by neglecting the untapered cylindrical section of the fiber and use a round table matching diamond dimensions to represent the tapered part. This approach captures the MW magnetic field disturbance from the fiber's tapered interface with the diamond. We evaluate the FDP's disturbance on MW magnetic field and transmission properties using three diamond sizes: 10 μm×10 μm×5 μm, 5 μm×5 μm×2.5 μm, and 2 μm×2 μm×1 μm. A reference line segment at a constant horizontal height of 10 μm from the CPW's upper surface is chosen. With each reference line's length double that of the diamond's horizontal size, we normalize the distance to account for different diamond sizes and plot the H_x distribution trend and ROC on a single graph. It is feasible given that H_x varies little over small dimensions above the CPW.

As shown in Fig. 3(c), H_x varies within 3 A/m. And when converted to ROC, the disturbance of the three FDP on MW magnetic field is less than 0.5%, lower than that of the bulk diamond. Similarly, as depicted in Fig. 3(d), FDPs of these sizes have a minimal impact on the CPW's S_{21}, less than 0.05%, which is considerably lower than the 2% observed with bulk diamond. This level of impact is negligible in practical applications. Moreover, the smaller the diamond, the lesser the effect on S_{21}. It is reasonable to conclude that submicron or nanoscale diamonds would have an insignificant effect on RF device transmission properties. Therefore, we conclude that FDP is superior to bulk diamond in terms of minimizing MW magnetic field disturbance and preserving transmission properties of RF devices.

4. Conclusion and perspectives

In this study, firstly the MW magnetic field of CPW is characterized and a good fit between the experiment and the simulation is obtained. Then we compare the disturbance induced by bulk diamond and tapered FDP on CPW. Our simulations demonstrate that the tapered FDP exerts minimal impact on the CPW's MW magnetic field ($< 0.5\%$) and S_{21} parameters ($< 0.05\%$), establishing its suitability for millimeter-wave applications. Notably, we observe that smaller diamond sizes at the fiber's end further reduce S_{21} disturbance, suggesting that submicron diamonds enhance spatial resolution and minimize interference with RF devices, resulting in more accurate measurements. Experimental validation corroborates these findings, confirming that these methods remain within acceptable error margins. Consequently, they offer lossless, high-resolution MW field measurement across various frequency

bands.

Acknowledgements

Project supported by the National Key Research and Development Program of China (Grant No. 2021YFB2012600). We acknowledge technical support by Tie-ying Feng of Jiangsu Institute of Metrology.

References

[1] Jennings J M, Kar A, Vaidyanathan R 2020 *AIP Advances* **10** 065202
[2] Wu J F, Zheng Y F, Liu P G, Dong M M and Du G X 2021 *Int. J. RF Microw. Comput. Aided. Eng.* **31** e22650
[3] Fancher C T, Scherer D R, John M C S and MarlowMauger B L S 2021 *IEEE Trans. Quantum Eng.* **2** 1
[4] Liu B, Zhang L H, Liu Z K, Deng Z A, Ding D S, Shi B S and Guo G C 2023 *Electromagnetic Science* **1** 1
[5] Kumar S, Fam H Q, Kübler H, Sheng J T and Shaffer J P 2017 *Sci. Rep.* **7** 42981
[6] Affolderbach C, Du G X, Bandi T, Horsley A, Treutlein P and Mileti G 2015 *IEEE Transactions on Instrumentation and Measurement* **64** 3629
[7] Beveratos A, Brouri R, Poizat J P and Grangier P 2002 *Quantum Communication, Computing, and Measurement* (New York: Springer) p. 261
[8] Appel P, Neu E, Ganzhorn M, Barfuss A, Batzer M, Gratz M, Tschöpe A and Maletinsky P 2016 *Rev. Sci. Instrum.* **87** 063703
[9] Pham L M, Sage D L, Stanwix P L, Yeung T K, Glenn D, Trifonov A, Cappellaro P, Hemmer P R, Lukin D M, Park H, Yacoby A and Walsworth R L 2011 *New J. Phys.* **13** 045021
[10] Epstein J R, Mendoza F M, Kato Y K and Awschalom D D 2005 *Nat. Phys.* **1** 94
[11] Gaebel T, Domhan M, Popa I, Wittmann C, Neumann P, Jelezko F, Rabeau J R, Stavrias N, Greentree A D, Prawer S, Meijer J, Twamley J, Hemmer P R and Wrachtrup J 2006 *Nat. Phys.* **2** 408
[12] Childress L I 2007 *Coherent manipulation of single quantum systems in the solid state*, Ph. D. Dissertation (Cambridge: Harvard University)
[13] Barson M S J, Oberg L M, McGuinness L P, Denisenko A, Manson N B, Wrachtrup J and Doherty M W 2021 *Nano Lett.* **21** 2962
[14] Appel1 P, Ganzhorn M, Neu E and Maletinsky P 2015 *New J. Phys.* **17** 112001
[15] Bai R X, Zhu X Y, Yang F, Gao T R, Wang Z R, Yu L Y, Wang J F, Zhou L and Du G X 2022 *Chin. Phys. B* **31** 074203
[16] Bai R X, Yang F, Liu P, Gao T R, Zhou L, Yin X H, Zhu X Y, Ma W H, He F Y, Chen N C, Sun Y, Ma J T, Yu T and Du G X 2022 *Appl. Phys. Lett.* **120** 044003
[17] Li M X, Zhang N, Xu L X, Zhang J X, Bian G D, Fan P C, Wang S X and Yuan H 2023 *Phys. Rev. Appl.* **19** 054088
[18] Chen G B, Gu B X, He W H, Guo Z G and Du G X 2020 *IEEE J. Quantum Electron.* **56** 1
[19] Wang Y P, Zhang R J, Yang Y, Wu Q, Yu Z F and Chen B 2023 *Chin. Phys. B* **32** 070301
[20] Ye J F, Jiao Z, Ma K, Huang Z Y, Lv H J and Jiang F J 2019 *Chin. Phys. B* **28** 047601
[21] Steiner M, Neumann P, Beck J, Jelezko F and Wrachtrup J 2010 *Phys. Rev. B* **81** 035205
[22] Dong M M, Hu Z Z, Liu Y, Yang B, Wang Y J and Du G X 2018 *Appl. Phys. Lett.* **113** 131105
[23] Duan D, Du G X, Kavatamane V K, Arumugam S, Tzeng Y K, Chang H C and Balasubramanian G 2019 *Opt. Express* **27** 6734